JOURNAL OF VIROLOGY, July 2008, p. 6161–6171 Vol. 82, No. 13
0022-538X/08/$08.00+0 doi:10.1128/JVI.02151-07

Interaction between Polypeptide 3ABC and the 5′-Terminal Structural Elements of the Genome of Aichi Virus: Implication for Negative-Strand RNA Synthesis▽

Shigeo Nagashima,† Jun Sasaki,* and Koki Taniguchi

Department of Virology and Parasitology, Fujita Health University School of Medicine, Toyoake, Aichi 470-1192, Japan

Received 1 October 2007/Accepted 23 April 2008

Secondary structural elements at the 5′ end of picornavirus genomic RNA function as *cis*-acting replication elements and are known to interact specifically with viral P3 proteins in several picornaviruses. In poliovirus, ribonucleoprotein complex formation at the 5′ end of the genome is required for negative-strand synthesis. We have previously shown that the 5′-end 115 nucleotides of the Aichi virus genome, which are predicted to fold into two stem-loops (SL-A and SL-C) and one pseudoknot (PK-B), act as a *cis*-acting replication element and that correct folding of these structures is required for negative-strand synthesis. In this study, we investigated the interaction between the 5′-terminal 120 nucleotides of the genome and the P3 proteins, 3AB, 3ABC, 3C, and 3CD, by gel shift assay and Northwestern analysis. The results showed that 3ABC and 3CD bound to the 5′-terminal region specifically. The binding of 3ABC was observed on both assays, while that of 3CD was detected only on Northwestern analysis. No binding of 3AB or 3C was observed. Binding assays using mutant RNAs demonstrated that disruption of the base pairings of the stem of SL-A and one of the two stem segments of PK-B (stem-B1) abolished the 3ABC binding. In addition, the specific nucleotide sequence of stem-B1 was responsible for the efficient 3ABC binding. These results suggest that the interaction of 3ABC with the 5′-terminal region of the genome is involved in negative-strand synthesis. On the other hand, the ability of 3CD to interact with the 5′-terminal region did not correlate with the RNA replication ability.

Picornaviruses include many human and animal pathogens such as poliovirus, rhinovirus, hepatitis A virus (HAV), and foot-and-mouth disease virus (33). Picornaviruses are small, nonenveloped, icosahedral viruses, the diameter of the particles being approximately 30 nm. The single-stranded, positive-sense RNA genomes of picornaviruses consist of 7,200 to 8,500 nucleotides (nt) and comprise a 5′ untranslated region (UTR), a single coding region, a 3′ UTR, and a poly(A) tail, from the 5′ end. The coding region encodes a long polyprotein that is cleaved into functional proteins by virus-encoded proteinases. Some of the polyprotein intermediates also have functions during viral replication. The positive-strand genomic RNA also serves as a template for the synthesis of negative-strand RNA, which is then transcribed into positive-strand RNA. The newly synthesized positive-strand RNA is encapsidated to form virions.

The 5′-terminal region of the picornavirus genomes folds into secondary or tertiary structures (33, 34) and functions as a *cis*-acting element for viral RNA replication (1, 5, 13, 20, 21, 26). In addition, it is reported that this region is involved in RNA stabilization and encapsidation (5, 36). This region is known to interact with host proteins and viral proteins, especially P3 cleavage products (33). The P3 proteins include 3A (membrane-associated protein), 3B (genome-linked protein, VPg), 3C protease, and 3D RNA-dependent RNA polymerase, and some of the precursors also have various functions (33). The 5′-end 90 nt of the poliovirus genome fold into a cloverleaf-like structure and form a ribonucleoprotein (RNP) complex through interaction with 3CD and a host protein, poly(rC)-binding protein (PCBP) (1, 2, 8, 29). Mutations that disrupt the cloverleaf structure inhibit the interaction with these proteins and reduce or completely abolish viral RNA replication (1, 2, 30). Thus, the formation of an RNP complex at the 5′ end of the poliovirus genome is essential for efficient RNA replication. The binding of 3AB promotes the interaction between the cloverleaf structure and 3CD (12, 39). Additionally, this 5′-end RNP complex interacts with the 3′ poly(A) tail through binding to poly(A)-binding protein (PABP), and formation of this circular RNP complex is required for the initiation of negative-strand RNA synthesis (5, 13, 19). In coxsackievirus B3 (CVB3) and rhinovirus 14, 3C interacts with the cloverleaf structure at the 5′ end of the genome (18, 28, 38, 42). For HAV, 3AB, 3ABC, 3C (15, 16, 31), and PCBP2 (10) have been shown to interact with the 5′-terminal 150 nt of the genome containing three stem-loop structures and a polypyrimidine-rich sequence. However, no direct evidence has been provided that the formation of an RNP complex is required for HAV RNA replication.

Aichi virus, which is associated with acute gastroenteritis in humans (40), is a member of the genus *Kobuvirus* of the family *Picornaviridae* (32, 41). We have already investigated the functions of the two stem-loops (SL-A and SL-C) and a pseudoknot structure (PK-B) predicted to be formed at the 5′ end of the genome and have shown that all of these structural elements are critical for viral RNA replication (24, 25, 35). In addition, using a cell-free translation-replication system, we have dem-

* Corresponding author. Mailing address: Department of Virology and Parasitology, Fujita Health University School of Medicine, Toyoake, Aichi 470-1192, Japan. Phone: 81-562-93-2486. Fax: 81-562-93-4008. E-mail: jsasaki@fujita-hu.ac.jp.

† Present address: Department of Hygiene, Sapporo Medical University School of Medicine, Sapporo, Hokkaido 060-8556, Japan.

▽ Published ahead of print on 30 April 2008.

TABLE 1. Sequences and positions of primers used for construction of plasmids

No.	Name	Sequence (5′–3′)[a]	Position
1	Eco-5700 P	(+) AAGAATTCGGCAACCGGGTCATCGAC	5700–5717
2	Hind-6066 M	(−) AAAAGCTT**TCA**CTGGCGCTGGATGTGACG	6048–6065
3	Hind-6635 M	(−) AAAAGCTT**TCA**TTGTTGGGTAGTGGCAAATTGAG	6613–6635
4	Csp45I-6478-3Cmut P	(+) CCTTCGAAGGTCTGgcCGGTTCCCCGCTTG	6478–6507
5	Eco-6066 P	(+) AAGAATTCGGAATCTCCCCTGCTGTCCCC	6066–6086
6	Hind-8042 M	(−) AAAAGCTT**TCA**GGCAGCCAGCAGATTTAG	8022–8042
7	Mlu-8044 P	(+) AAACGCGTAGTTAGGGAACACAGTGCCT	8044–8063
8	Sal-IRES-3′ M	(−) AAAGTCGACATAAAAGGATTGGAAATGAAA	714–734
9	Sal-Met-5700 P	(+) AAGTCGACGTC**ATG**GGCAACCGGGTCATCGACGCG	741–746 and 5700–5720
10	Mlu-Stop-8039 M	(−) AAACGCGT**TTA**GGCAGCCAGCAGATTTAGC	8021–8039
11	Mlu-Stop-6635 M	(−) AAACGCGT**TTA**TTGTTGGGTAGTGGCAAAT	6617–6635

[a] The restriction enzyme sites are underlined; the initiation or stop codons are indicated by bold; the mutated nucleotides are indicated by lowercase letters.

onstrated that the 5′ end of the Aichi virus genome is involved in both positive- and negative-strand RNA synthesis and that disruption of the predicted base pairings of the stem segments of the structural elements prevents negative-strand RNA synthesis (25).

In this study, we investigated the interaction between the 5′-terminal region of the Aichi virus genome and viral P3 proteins by gel shift assay and Northwestern assay. The results showed that 3ABC and 3CD bound to the 5′-terminal region specifically. 3AB and 3C did not interact with the 5′ end of the genome. Disruption of the predicted base pairings in the stem of SL-A and stem-B1 inhibited the binding of 3ABC to the 5′ end of the genome. Thus, interaction between 3ABC and the 5′-terminal RNA structures was suggested to be involved in negative-strand synthesis. On the other hand, the ability of 3CD to interact with the 5′-terminal region did not correlate with the RNA replication ability.

MATERIALS AND METHODS

Plasmids. The 3AB, 3ABC, 3C, and 3CD coding regions were amplified by PCR with primer pairs 1 and 2, 1 and 3, 3 and 5, and 5 and 6 (Table 1), respectively, using pAV-FL, an infectious cDNA clone of Aichi virus (35), as the template. The PCR products were cloned into the pCRII-TOPO vector (Invitrogen) and sequenced. These derived plasmids were called pCR-3AB, pCR-3ABC, pCR-3C, and pCR-3CD, respectively. The EcoRI-HindIII fragments of pCR-3AB and pCR-3C were ligated into the same sites of pMAL-c2X (New England Biolabs), which provided an N-terminal maltose binding protein (MBP) on each protein. These derived plasmids were called pMAL-3AB and pMAL-3C, respectively. To introduce mutations (T6492G and G6493C) changing the cysteine at the active site of the 3C protease of the 3ABC and 3CD coding regions to alanine (11), PCR-based mutagenesis was performed with primer pair 3 and 4 and pair 4 and M13-20, which anneals to the vector sequence downstream of the poly(A) tract in pAV-FL (Table 1), respectively, using pAV-FL as the template. The PCR fragments were cloned into the pCRII-TOPO vector and sequenced; the Csp45I-HindIII and Csp45I-PstI fragments carrying the mutations were replaced with the corresponding fragments of pCR-3ABC and pCR-3CD, generating pCR-3ABCmut and pCR-3CDmut, respectively. The EcoRI-HindIII fragments containing the whole 3ABC and 3CD coding sequences were cut out from pCR-3ABC-mut and pCR-3CDmut, respectively, and ligated into the same sites of pMAL-c2X, yielding pMAL-3ABCmut and pMAL-3CDmut.

The coding region (741 to 8043) of pAV-FL was deleted by inverse PCR with primer pair 7 and 8 (Table 1), and the derived plasmid, pAV-FLΔ741–8043, was used as a cassette plasmid for Aichi virus internal ribosome entry site-dependent expression of the P3 and 3ABC proteins in Vero cell S10 extracts. The P3 coding region was amplified by PCR with primer pair 9 and 10 (Table 1), using pAV-FL as the template. The 3ABC coding region was amplified by PCR with primer pair 1 and 11 (Table 1), using pCR-3ABCmut as the template. Each PCR product was cloned into the pCRII-TOPO vector and sequenced, and then the SalI-MluI fragment containing the coding region of each clone was ligated into the same sites of pAV-FLΔ741–8043. The derived clones were called pAV-IRES-P3 and pAV-IRES-3ABCmut.

Expression and purification of recombinant proteins. All recombinant proteins were expressed in *Escherichia coli* (DH5α) and purified according to the manufacturer's recommended protocol (New England Biolabs). *E. coli* cells transformed with pMAL-c2X, which expressed MBP, pMAL-3AB, pMAL-3AB-Cmut, pMAL-3C, or pMAL-3CDmut, were grown at 37°C in rich broth containing glucose and ampicillin until the optical density at 600 nm reached 0.5. Isopropyl-β-D-thiogalactoside (IPTG) was added to the culture to a final concentration of 0.3 mM, and then the cells were cultured further for 2 h. The cells were harvested, suspended in column buffer (20 mM Tris-HCl [pH 7.4], 200 mM NaCl, 1 mM EDTA), and then lysed by three consecutive freeze-thaw cycles. The lysates were sonicated for 3 min in total and centrifuged, and then the supernatant (crude extract) was diluted and loaded onto an amylose resin column (New England Biolabs). The column was washed with the column buffer, and then the fusion proteins were eluted with the column buffer containing 10 mM maltose. Fractions were collected, and the purified fusion proteins were analyzed by sodium dodecyl sulfate (SDS)-polyacrylamide gel electrophoresis (PAGE) and visualized by Coomassie brilliant blue (CBB) staining. MBP was removed from the MBP fusion proteins by digestion with factor Xa.

RNA translation in Vero cell S10 extracts. The standard reaction was carried out as described previously (25). A 10-μl reaction mixture containing 100 ng of RNA transcripts and 2 μCi of [^{35}S]methionine-cysteine (Amersham) was incubated at 32°C. At various times during the incubation, 2 μl of the reaction mixture was subjected to SDS-12% PAGE, and then the gel was dried and exposed to a FujiFilm imaging plate. Radioactive signals were detected with a BAS2000 (FujiFilm).

5′ UTR cloning. The first 120 nt of the 5′ UTR were amplified by PCR with primers M13-RV, which anneals with the vector sequence upstream of the T7 promoter sequence in pAV-FL, and Hind-SP6-120 M (5′ AAAAGCTTatttaggt gacactatagGGTGCCCGTTTAATTCCTCCG; minus sense; from nt 99 to 119, with the HindIII site underlined and the SP6 promoter sequence indicated by lowercase letters), using pAV-FL as the template. The PCR product was digested with EcoRI and HindIII and then cloned into the same sites of pUC118. The derived plasmid was called pAV-5′-120. The 5′-end 120 nt of mut4, mut5, mut6, mutB-1, mutB-2, mutB-3, mutB-4, and mutC-7, respectively, were amplified by PCR with primers M13-RV and Hind-SP6-120 M using each mutant plasmid constructed in our previous studies (24, 35) as the template. The PCR products were digested with EcoRI and HindIII and then cloned into the same sites of pUC118. The 5′-UTR clone of mut112-118, which was constructed in the previous study (25), was obtained by inverse PCR as described previously (35), using pAV-5′-120 as the template. The sequences of the primers used are as follows: 119-SP6-Hind P (5′ CctatagtgtcacctaaatAAGCTT; plus sense; nt 119, with the HindIII site underlined) and mut112-118 M (5′ CACGAGCTTTAAT TCCTCCGAACAGGTTCC; minus sense; from nt 89 to 118, with the mutations underlined). The PCR product was self-ligated.

In vitro transcription. pAV-5′-120 and its mutants were linearized by digestion with HindIII. To synthesize competitor RNA consisting of 100 nt of the pGEM vector sequence, the pGEM vector was linearized by digestion with MluI. RNA transcripts were synthesized with T7 RNA polymerase using a T7 RiboMAX Express large-scale RNA production system (Promega). The integrity of the synthesized RNAs was confirmed by agarose gel electrophoresis.

Preparation of RNA probes. Labeled RNA probes were synthesized with T7 RNA polymerase, using a Maxiscript kit (Ambion) and [α-^{32}P]CTP, according to the

manufacturer's recommended protocol. DNA templates were amplified by PCR with primers M13 reverse primer and 120 M (5′ GGGTGCCCGTTTAATTCC TCC; minus sense; from nt 100 to 120) from pAV-5′-120 and all of its mutants except for mut112-118. For amplification of the DNA template from mut112-118, primer 120-mut112-118 M (5′ GGCACGAGCTTTAATTCCTCCGAACAGGT; minus sense; from nt 92 to 120, with the mutations underlined) was used instead of 120 M. RNA transcripts were synthesized with T7 RNA polymerase using 0.2 μg of each purified DNA template; 165 nM [α-^{32}P]CTP; 5 μM CTP; and 500 μM each of ATP, GTP, and UTP. To synthesize the labeled RNA comprising 100 nt of the pGEM vector sequence, 1 μg of the pGEM vector linearized by digestion with MluI was used as the template. Unincorporated labeled nucleotides were removed with Probequant G-50 microcolumns (Amersham Bioscience). The integrity of the synthesized RNAs was confirmed by 5% acrylamide-8 M urea gel electrophoresis. The gel was dried, and radioactive signals were detected with a BAS2000 (FujiFilm).

Gel shift assay and competition assay. The gel shift assay was carried out according to the method of Kusov and Gauss-Muller (16) with some modifications. The [α-^{32}P]CTP-labeled RNA probe was diluted in nuclease-free water and then incubated at 45°C for 30 min before being added to the binding reaction mixture. The binding reaction mixture (50 μl) contained 5 mM HEPES-KOH (pH 7.9), 25 mM KCl, 2 mM $MgCl_2$, 5% glycerol, 6 mM dithiothreitol (DTT), 1.75 mM ATP, 0.05 mM phenylmethylsulfonyl fluoride, 8 μg of *E. coli* tRNA, ^{32}P-labeled RNA (100,000 cpm), RNasin (20 U), and a purified recombinant viral protein (~2 μM). The binding reaction mixture was preincubated with a purified protein at 30°C for 5 min, and then the ^{32}P-labeled RNA probe was added and the incubation was continued for an additional 20 min. Ten microliters of RNA dye containing 1 mM EDTA, 0.25% bromophenol blue, 0.25% xylene cyanol, and 50% glycerol was added to the binding reaction mixture, and the binding reactions were analyzed on a 5% native polyacrylamide gel (acrylamide to bisacrylamide ratio of 79:1) with 0.5× TBE (45 mM Tris, 44 mM boric acid, and 1 mM EDTA [pH 8.3]) at 4°C. The gels were prerun for 1 h at 100 V, the binding reaction mixtures were then loaded, and electrophoresis was continued at 300 V for 2 h 30 min. The gel was dried, and radioactive signals were detected as described above. In competition experiments, unlabeled RNA competitors (5 μg) were mixed with [α-^{32}P]CTP-labeled RNA prior to addition to the binding reaction mixture.

Northwestern blot analysis. Northwestern blot analysis was performed as described by Kusov and Gauss-Muller (16) with modifications. Purified Aichi virus 3AB, 3ABC, 3C, and 3CD (approximately 0.5 μg); MBP; or each MBP fusion protein (approximately 1 μg) was subjected to SDS-PAGE and then blotted onto a polyvinylidene difluoride (PVDF) membrane (Bio-Rad). The membrane was blocked at room temperature for 1 h with phosphate-buffered saline containing 5% nonfat milk and 1 mM DTT and then washed with 1× HBB (25 mM HEPES-KOH [pH 7.5], 25 mM NaCl, 5 mM $MgCl_2$, and 1 mM DTT). The transferred proteins were renatured by consecutive washes (15 min each at room temperature) with 6, 3, 1.5, 0.75, 0.375, 0.187, and 0 M guanidinium hydrochloride in 1× HBB. The membrane was washed twice with 1× HYB (20 mM HEPES-KOH [pH 7.5], 100 mM KCl, 2.5 mM $MgCl_2$, 0.1 mM EDTA, 0.05% Nonidet P-40, and 1 mM DTT) and once with 1× HYB containing *E. coli* tRNA (1 μg/ml). The ^{32}P-labeled RNA probe (200,000 cpm) in 1× HYB containing RNasin (1 U/ml) and tRNA (1 μg/ml) was incubated with the renatured membrane-bound proteins for 1 h at room temperature and then overnight at 4°C. The unbound probe was removed by three washes with 1× HYB or 1× HYB containing 200 mM NaCl. The membrane was dried at room temperature, and signal intensities were measured with a BAS2000.

RESULTS

Interaction between bacterially expressed P3 nonstructural proteins of Aichi virus and the 5′-terminal region of the genome. Previous studies showed that two stem-loops (SL-A and SL-C) and one pseudoknot structure predicted to be formed within the 5′-end 115 nt of the Aichi virus genome (Fig. 1A) are critical for viral RNA replication (24, 25, 35). The previously unnamed pseudoknot structure, which is formed through a base-pairing interaction between the loop segment (nt 57 to 60) of the stem-loop (previously termed SL-B) and the sequence downstream of SL-C (nt 112 to 115), is designated PK-B, and the two stem segments of PK-B are termed stem-B1 (nt 45 to 52/61 to 68) and stem-B2 (nt 57 to 60/112 to 115). Here we examined whether the P3 nonstructural proteins interact with the 5′-terminal region containing these structural elements.

When the P3 region was expressed in Vero cell S10 extracts, several bands were observed besides those of P3, 3CD, 3D, 3C, and 3AB (Fig. 2B, lane 1). One of these proteins was thought to be 3ABC, since its electrophoretic mobility was the same as that of 3ABC, which was expressed solely from AV-IRES-3ABCmut RNA (lane 2). Also, on translation of the full-length viral RNA (AV-FL RNA) in Vero cell S10 extracts, in addition to 3CD, 3D, 3AB, and 3C, 3ABC was found, albeit as a relatively less abundant polyprotein intermediate (lanes 3 to 5). Based on this finding, 3AB, 3ABC, 3C, and 3CD were subjected to binding assays in this study.

3AB, 3ABC, 3C, and 3CD were expressed as fusion proteins with MBP in *E. coli* (Fig. 2A). For 3ABC and 3CD, mutations (T6492G and G6493C) were introduced to abolish the 3C protease activity (11). The MBP fusion proteins were purified using amylose resin, and the identity of the purified proteins was confirmed by CBB staining following separation by SDS-PAGE (Fig. 2C). The molecular masses of the purified proteins corresponded to those expected for each viral protein plus an MBP: MBP, 43 kDa; MBP-3AB, 57 kDa; MBP-3ABC, 77 kDa; MBP-3C, 63 kDa; MBP-3CD, 110 kDa. Furthermore, MBP was removed from the fusion proteins by digestion with factor Xa, and then the sizes of the separated viral proteins were confirmed (data not shown).

Through the gel shift assay, we investigated the interactions between the purified MBP fusion proteins and an [α-^{32}P]CTP-labeled RNA probe consisting of the 5′-end 120 nt of the Aichi virus genome. When the labeled RNA probe was electrophoresed on a nondenaturing gel, two slower-migrating bands were observed (Fig. 3A, lane 1). These could be due to distinct conformations of the RNA probe, since the RNA probe migrated as a single band in a denaturing gel (data not shown). Incubation of the RNA probe with MBP-3ABC resulted in the appearance of a slow-migrating band representing the formation of an RNP complex (Fig. 3A, lanes 6 and 7). The amount of the RNP complex formed increased depending on the concentration of MBP-3ABC (Fig. 3B). When the RNA probe was incubated with the other proteins, MBP-3AB, MBP-3C, MBP-3CD, or MBP, no complex was observed (Fig. 3A, lanes 2 to 5 and 8 to 11). Even when these proteins were used at higher concentrations, no RNP complex was formed (data not shown).

To determine whether the binding of the MBP-fusion proteins to the RNA probe was influenced by the fused MBP sequence, the gel shift assay was carried out using the viral proteins separated from MBP by digestion with factor Xa. Consistent with the results of the assay using the MBP fusion proteins, 3ABC formed an RNP complex with the 5′ end of the genome (Fig. 3C, lane 4), whereas 3AB, 3C, and 3CD were unable to shift the mobility of the RNA probe.

To determine whether the interaction of MBP-3ABC with the RNA probe consisting of the 5′-end 120 nt of the genome is specific, a competition experiment was carried out using unlabeled homologous or unrelated RNAs. An excess of an unlabeled homologous RNA abolished the shift of the labeled RNA probe (Fig. 3D, lane 3). In contrast, the RNP complex formation was unaffected by the unrelated compet-

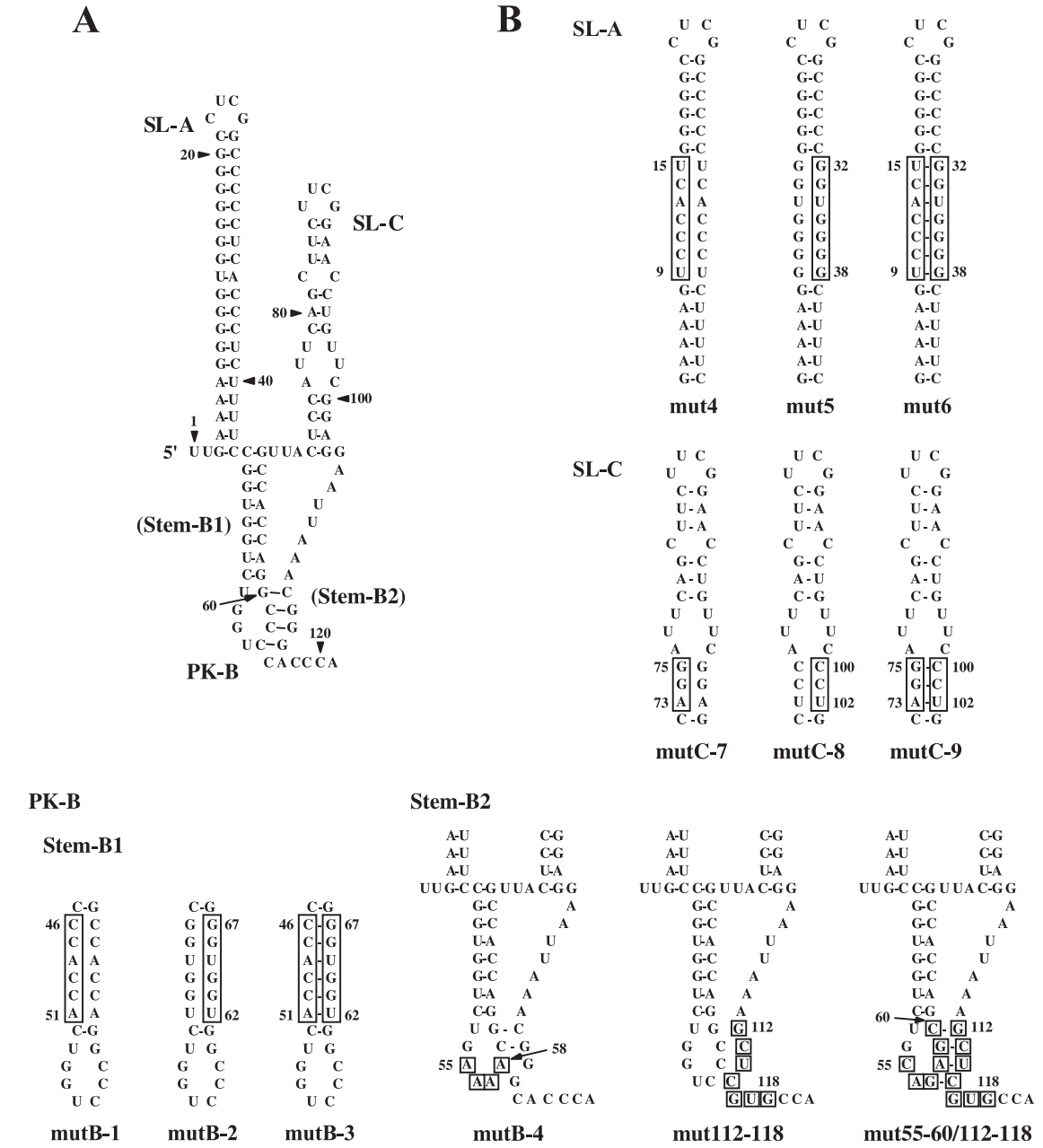

FIG. 1. (A) The two stem-loops (SL-A and SL-C) and one pseudoknot structure (PK-B) within the 5′-end 115 nt of the Aichi virus genome. (B) Site-directed mutations introduced into SL-A, SL-C, and PK-B. The mutated regions are boxed. The 5′-end 120-nt sequences containing these mutations were used in RNA-protein binding assays.

itor RNA derived from the sequence of the pGEM vector (Fig. 3D, lane 4).

Thus, in the gel shift assay, only 3ABC among the P3 proteins examined showed a specific interaction with the 5′-end 120 nt of the genome.

Northwestern blot analysis of the interaction between the 5′ end of the genome and P3 proteins. The interactions between the 5′ end of the genome and the P3 proteins were analyzed using another method, Northwestern blot analysis. MBP-3AB, MBP-3ABC, MBP-3C, and MBP-3CD were subjected to SDS-PAGE, blotted onto a PVDF membrane, and then probed with labeled RNA (AV-5′-120) consisting of the 5′-end 120 nt of the genome. As a control probe to distinguish specific from nonspecific binding, we used an unrelated RNA consisting of the 100 nt of the pGEM vector sequence. The AV-5′-120 probe bound to MBP-3ABC (Fig. 4A). In addition, the AV-5′-120 probe showed weak binding to MBP-3CD. On the other hand, the control pGEM vector RNA did not bind to any MBP fusion protein (Fig. 4A). Similar results were obtained using viral proteins separated from MBP (Fig. 4B).

To further investigate the difference in RNA binding affinity between 3ABC and 3CD, the sensitivity of the RNP

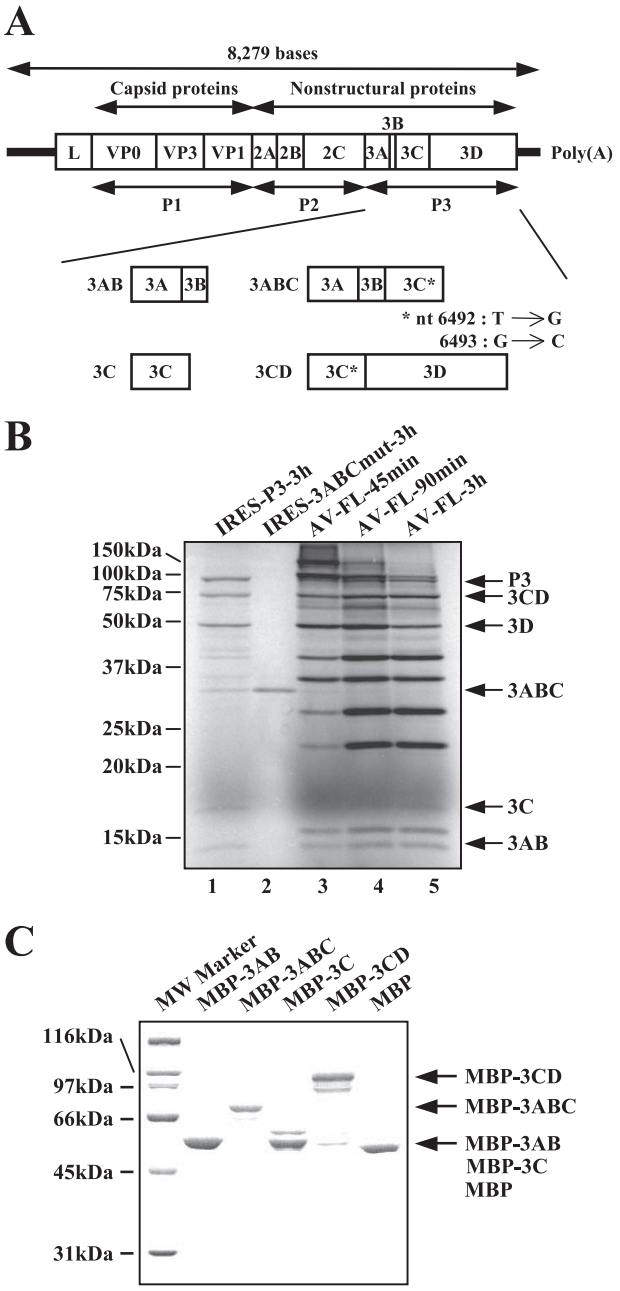

FIG. 2. (A) Schematic diagram of the Aichi virus genome and the P3 nonstructural proteins (3AB, 3ABC, 3C, and 3CD) expressed as MBP fusion proteins in *E. coli* in this study. The thick lines and open box indicate the UTRs and the coding region, respectively. Vertical lines within the box represent putative cleavage sites for viral protease. The asterisks indicate mutations (T6492G and G6493C) introduced into the 3C protease region to abolish the protease activity. (B) Expression of viral proteins in Vero cell S10 extracts. RNA transcripts were subjected to an in vitro translation reaction in the presence of [^{35}S]methionine-cysteine for the indicated times at 32°C. The translation products were electrophoresed on an SDS-polyacrylamide gel, and then the gel was dried. Radioactive signals were detected with a phosphorimager. The positions of molecular mass markers and each processed P3 protein are indicated on the left and right, respectively. (C) Fusion proteins of MBP with P3 nonstructural proteins, MBP-3AB, MBP-3ABC, MBP-3C, and MBP-3CD, and MBP were bacterially expressed, purified, and analyzed by SDS-PAGE followed by CBB staining. The positions of molecular mass markers and each purified MBP fusion protein are indicated on the left and right, respectively.

complex formation to the salt concentration was examined (7, 14, 22). MBP-3ABC and MBP-3CD were electrophoresed on SDS-polyacrylamide gels and then blotted onto PVDF membranes. The blotting efficiency was checked by CBB staining (Fig. 4C). After incubation with the RNA probe, the membranes were washed with a membrane washing solution containing different concentrations of NaCl (0 mM and 200 mM). Binding of the AV-5′-120 probe to MBP-3CD was weaker at 200 mM NaCl than at 0 mM NaCl, while the RNA binding activity of MBP-3ABC was hardly affected by the salt concentration (Fig. 4D). Thus, the binding of 3CD to the 5′-terminal sequence was more sensitive to the salt concentration than that of 3ABC.

3ABC specifically binds to SL-A and stem-B1. We have already carried out site-directed mutational analysis of the 5′-end region of the genome and obtained various mutants that could not synthesize negative-strand RNA in a cell-free replication system (24, 25, 35). In this study, to examine the relationship between the formation of an RNP complex at the 5′ end of the genome and negative-strand RNA synthesis, we investigated the abilities of 3ABC to bind to the 5′-end sequences of such mutants. mut5, mutB-1, mutB-4, mutC-7, and mut112-118 were used for this experiment (Fig. 1B). mut5 contains a 7-nt mutation (nt 32 to 38) in the middle part of the stem of SL-A to disrupt the base pairings of the stem (35). mutC-7 contains mutations that disrupt the base pairings of the lower stem of SL-C (24). In mutB-1, the base pairings of stem-B1 of PK-B were disrupted, while in mutB-4 and mut112-118, the formation of stem-B2 was prevented (24, 25). These mutants did not replicate in transfected cells and had a defect in negative-strand RNA synthesis in the cell-free translation-replication system (25).

Through the gel shift assay, we examined the competitive effect of the 5′-end 120 nt of mutant RNAs on the interaction of those of the wild-type genome with MBP-3ABC. The wild-type competitor RNA completely inhibited the formation of an RNP complex between the labeled wild-type RNA probe and MBP-3ABC (Fig. 5A, lane 3). mutB-4, mutC-7, and mut112-118 also showed inhibitory effects; however, their effects appeared to be slightly weaker than that of the wild-type competitor RNA, since small amounts of the RNP complex were still formed (Fig. 5A, lanes 6 to 8). On the other hand, mut5 or mutB-1 did not compete with the wild-type RNA probe (Fig. 5A, lanes 4 and 5).

Furthermore, Northwestern blot analysis was performed. As shown in Fig. 5B, the labeled probes consisting of the 5′-end 120 nt of mutB-4, mutC-7, and mut112-118 bound to MBP-3ABC, and their binding signals were weaker than that observed for the wild-type probe (compare lanes 1, 4, 5, and 6). On the other hand, interaction of the mut5 and mutB-1 probes with MBP-3ABC was not observed (Fig. 5B, lanes 2 and 3).

Considering that the base pairings of the stem of SL-A and stem-B1 were disrupted in mut5 and mutB-1, respectively, these results indicate that SL-A and stem-B1 are major determinants of the binding of 3ABC.

3ABC binding requires the proper formation of the stem of SL-A and stem-B1. To determine whether loss of the binding activity to 3ABC observed for mut5 and mutB-1 is due to a change in the nucleotide sequence or to disruption of the base

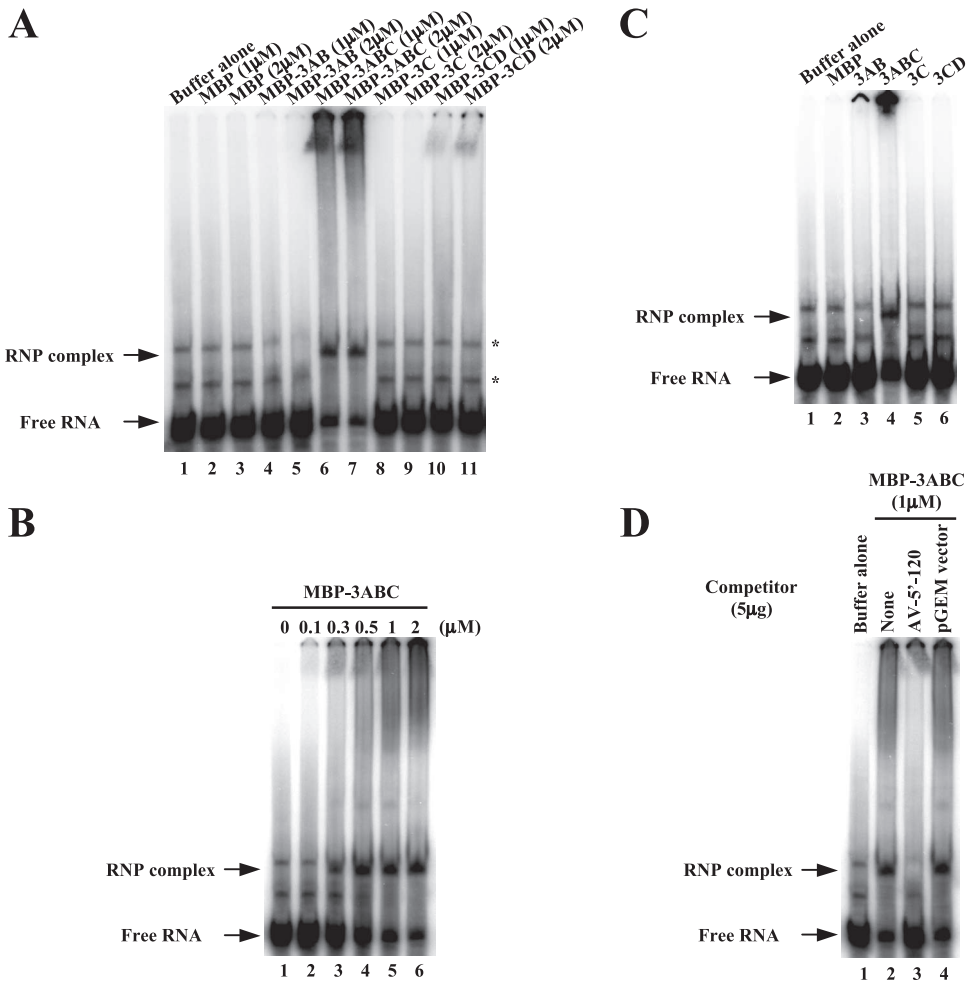

FIG. 3. Gel shift assay of the interactions of the recombinant P3 proteins with an RNA probe consisting of the 5′-end 120 nt of the genome. (A) The labeled RNA probe was incubated with purified MBP-3AB, MBP-3ABC, MBP-3C, MBP-3CD, or MBP to form an RNA-protein complex. The resulting complexes were analyzed by nondenaturing 5% PAGE. Radioactive signals were detected with a phosphorimager. The positions of free RNA and RNP complex are indicated. The asterisks indicate altered migration of the RNA probe. (B) The interaction of the RNA probe with increasing amounts of purified MBP-3ABC. (C) The interaction of the labeled RNA probe with the purified P3 nonstructural proteins (3AB, 3ABC, 3C, and 3CD) separated from MBP. (D) Competition experiment between the labeled RNA probe and the unlabeled viral 5′-terminal RNA (AV-5′-120) or unrelated RNA (pGEM vector sequence) for MBP-3ABC binding. Purified MBP-3ABC was incubated with the labeled RNA probe and competitor RNAs to form an RNA-protein complex.

pairings of the stem, we analyzed other mutants of SL-A or stem-B1.

For SL-A, mut4, mut5, and mut6 were used for this experiment (Fig. 1B). mut4 contains mutations that disrupt the base pairings of the stem of SL-A. In mut6, 7-nt stretches (nt 9 to 15 and 32 to 38) in the stem of SL-A are exchanged with each other to maintain the base pairings of the stem of SL-A. mut5 was described above. The previous study showed that mut4 RNA is unable to replicate in transfected cells, while mut6 RNA replicates as well as the wild type does (35). By using unlabeled RNAs consisting of the 5′-end 120 nt of these mutants as competitors, the binding of the labeled wild-type RNA probe to 3ABC-MBP was investigated by the gel shift assay. mut4, as well as mut5, did not inhibit the formation of the RNP complex (Fig. 6A, lanes 4 and 5). In contrast, the competitor mut6 RNA abolished the interaction between the wild-type RNA probe and MBP-3ABC (Fig. 6A, lane 6). On Northwestern blot analysis, the mut6 RNA probe, but not the mut4 or mut5 probe, bound to MBP-3ABC (Fig. 6B). These results indicate that formation of the base pairings of the stem of SL-A is important for the binding of 3ABC.

Similarly, mutants of stem-B1 of PK-B, mutB-1, mutB-2, and mutB-3, were analyzed (Fig. 1B). mutB-1 was described above. mutB-2 contains mutations that disrupt the base pairings of stem-B1. mutB-3 was constructed by exchanging the 6-nt stretches (nt 46 to 51 and 62 to 67) in stem-B1 with each other to maintain the base pairings. In the previous study, mutB-2 was shown not to replicate in transfected cells (24). On the other hand, mutB-3 RNA could replicate and generate viable viruses in transfected cells, although the RNA replication efficiency and virus titer were 24 to 40% and 100-fold lower than those of the wild type, respectively (24). The gel shift assay was carried out using unlabeled RNAs consisting of the 5′-end 120 nt of these mutants as compet-

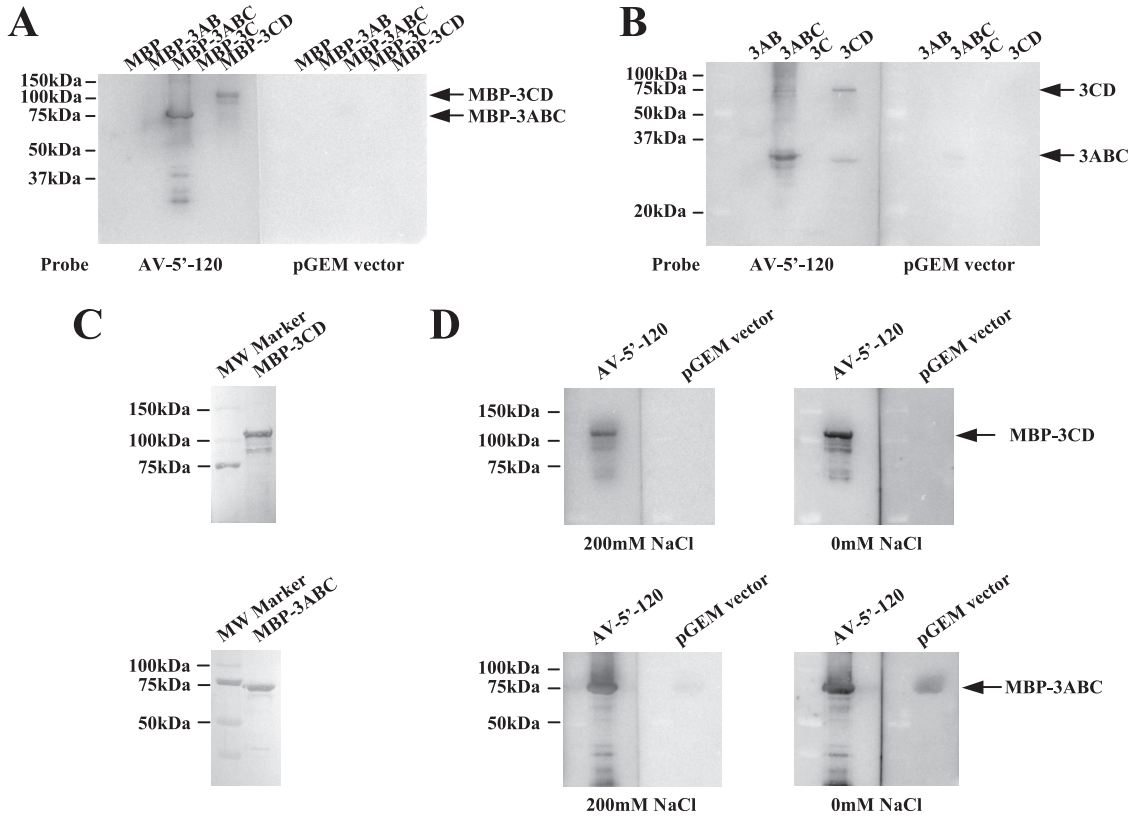

FIG. 4. Northwestern blot analysis of the interactions of the recombinant P3 proteins with the RNA probe consisting of the 5′-end 120 nt of the genome. (A and B) Purified MBP fusion proteins (A) or purified P3 proteins dissociated from MBP (B) were separated by SDS-PAGE, transferred to a PVDF membrane, renatured by incubation with decreasing amounts of guanidinium hydrochloride, and then probed with the labeled viral 5′-terminal RNA (AV-5′-120) or unrelated RNA (pGEM vector sequence). Radioactive signals were detected with a phosphorimager. The positions of molecular mass markers and the detected P3 proteins are indicated on the left and right, respectively. (C) The purified MBP-3ABC and MBP-3CD were separated by SDS-PAGE and transferred to a PVDF membrane, and then the membrane was stained with CBB. The positions of molecular mass markers are indicated on the left. (D) Effect of the NaCl concentration on RNP complex formation. The assay of binding of MBP-3ABC and MBP-3CD blotted on a PVDF membrane to the indicated RNA probes was performed as described above. The PVDF membrane was then washed with a membrane washing solution with or without 200 mM NaCl. The positions of molecular mass markers and of purified MBP-3ABC and MBP-3CD are indicated on the left and right, respectively.

itors. The results showed that the competitor mut-B1 and mutB-2 RNAs did not affect the interaction of the wild-type RNA probe with MBP-3ABC (Fig. 6C, lanes 4 and 5). In contrast, the competitor mutB-3 RNA showed a competitive effect, although a small amount of the RNP complex was formed (Fig. 6C, lane 6). On Northwestern blot analysis, only mutB-3 RNA among the three mutant RNA probes interacted with MBP-3ABC (Fig. 6D); however, the signal intensity with the mutB-3 probe was threefold weaker than that with the wild-type probe (Fig. 6D, compare lanes 1 and 4). These results indicate that the formation of the base pairings of stem-B1 is essential for the binding of 3ABC. In addition, the specific nucleotide sequence of stem-B1 was suggested to be required for efficient 3ABC binding.

Taken together, these results indicate that the proper formation of the stems of both SL-A and stem-B1 is a major determinant of the interaction between 3ABC and the 5′ end of the genome and that the specific nucleotide sequence of stem-B1 has a role in the binding to 3ABC. In addition, it was observed that the binding activity of 3ABC to the 5′ end of the wild-type and the mutant RNAs correlated well with the RNA replication efficiency.

Northwestern blot analysis of the interaction between the mutant RNAs and 3CD. To investigate further the binding property of 3CD to the 5′-terminal region of the genome, Northwestern analysis was performed using various mutant RNA probes which contain a single or double mutation to disrupt or restore the base pairings of either of the stem segments (Fig. 1B). For the stem segment of SL-C and stem-B2, efficient 3CD binding required maintenance of the base pairings of the stem segment (Fig. 7A, lanes 5 and 7). For SL-A, all of the introduced mutations reduced 3CD binding (Fig. 7B, lanes 2 to 4). For stem-B1, one single mutant (mutB-2) bound to 3CD efficiently, and another single mutant (mutB-1) and a double mutant (mutB-3) showed only weak binding (Fig. 7B, lanes 6 to 8). It is notable that the binding abilities of mut6 and mutB-3 probes were as weak as those of mut5 and mutB-1 probes, because the previous studies have shown that while the mutations introduced into mut6 and mutB-3 do not affect RNA replication, those introduced into mut5 and mutB-1 abolish it (24, 35). In addition, mutB-2 probe

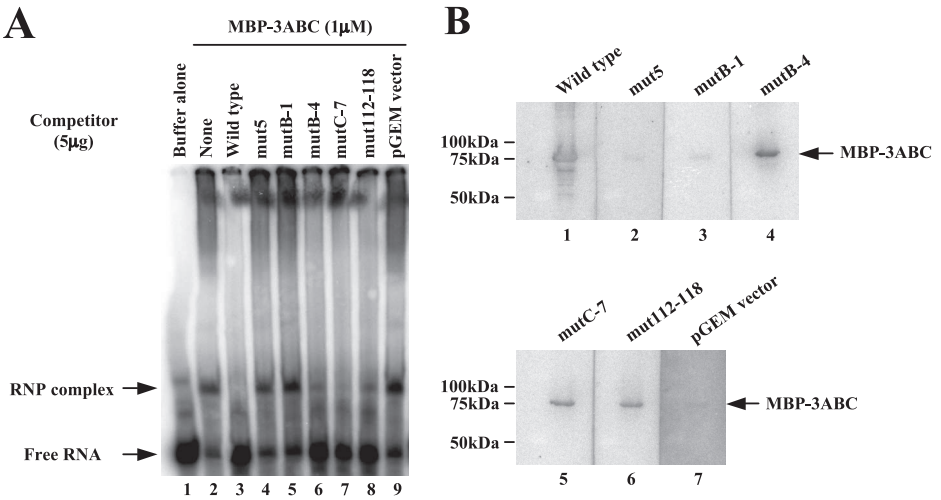

FIG. 5. (A) Gel shift competition experiment. The labeled probe corresponding to the 5′-end 120 nt of the wild-type genome was incubated with MBP-3ABC and each of the unlabeled competitors consisting of the 5′-end 120 nt of the indicated mutants. As control competitor RNAs, unlabeled homologous (wild type) or unrelated (pGEM vector) RNAs were used. The positions of free RNA and RNP complex are indicated. (B) Northwestern blot analysis of the interaction of MBP-3ABC with the RNA probe consisting of the 5′-end 120 nt of the wild-type genome or the mutants or with a control RNA probe derived from the pGEM vector. The positions of molecular mass markers and purified MBP-3ABC are indicated on the left and right, respectively.

exhibited efficient binding, although the mutation introduced into this probe has been shown to abolish RNA replication (24). These results suggest that the RNA replication ability is independent of the ability of 3CD to bind to the 5′-terminal RNA.

DISCUSSION

The 5′-terminal region of picornavirus genomes functions as a *cis*-acting RNA replication element (1, 5, 13, 20, 21, 26). This

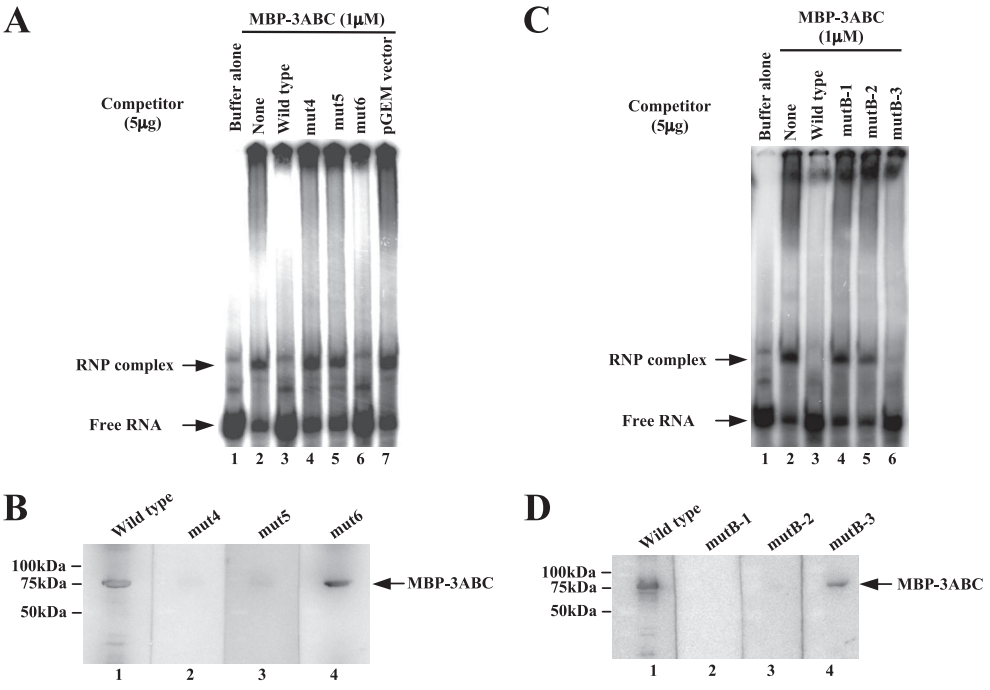

FIG. 6. The effect of the mutations introduced into SL-A (A and B) or stemB-1 (C and D) on the interaction with 3ABC. (A and C) Gel shift competition experiment. The labeled probe corresponding to the 5′-end 120 nt of the wild-type genome was incubated with MBP-3ABC and each of the unlabeled competitors consisting of the 5′-end 120 nt of the indicated mutants. As control competitor RNAs, the 5′-terminal 120-nt wild-type sequence and the pGEM vector sequence were used. The positions of free RNA and RNP complex are indicated. (B and D) Northwestern blot analysis of the interaction of MBP-3ABC with the RNA probe consisting of the 5′-end 120 nt of the wild-type genome or the mutants. The positions of molecular mass markers and purified MBP-3ABC are indicated on the left and right, respectively.

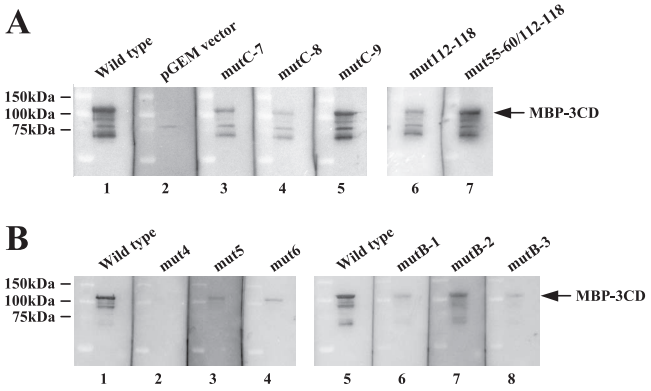

FIG. 7. Effect of the mutations introduced into SL-C or stem-B2 (A) or SL-A or stem-B1 (B) on the interaction with 3CD. Northwestern blot analysis of the interaction of MBP-3CD with the RNA probe consisting of the 5′-end 120 nt of the wild-type genome or the mutants. The positions of molecular mass markers and purified MBP-3CD are indicated on the left and right, respectively.

region has been reported to interact with P3 proteins in several picornaviruses; for example, 3CD of poliovirus (1, 2, 12); 3C of CVB3 (28, 42) and human rhinovirus 14 (18, 38); and 3ABC, 3AB, and 3C of HAV (15, 16, 31). We have previously shown that the 5′-end 115 nt of the Aichi virus genome, which are predicted to form two stem-loops and one pseudoknot, function as a *cis*-acting RNA replication element (24, 25, 35). In this study we investigated the interaction between the 5′-terminal region of the Aichi virus genome and the P3 proteins, 3AB, 3ABC, 3C, and 3CD, by gel shift assay and Northwestern blot analysis (Fig. 3 and 4). Among the P3 proteins examined, 3ABC and 3CD bound to the 5′-terminal region specifically. The binding of 3ABC was observed on both assays, while that of 3CD was detected only on Northwestern analysis.

In poliovirus, 3AB and 3CD are the primary cleavage products of the P3 region of the polyprotein, these intermediate cleavage products having been found to be relatively stable (12, 17). In contrast, in the P3 domain of the HAV polyprotein, polypeptide 3ABC is a relatively abundant intermediate (37). We examined processing of the Aichi virus polyprotein using Vero cell S10 extracts. 3AB and 3CD appeared to be the relatively abundant intermediates of P3 in Aichi virus, and 3ABC was found as a relatively less abundant intermediate (Fig. 2, lanes 3 to 5).

Like HAV 3ABC (15, 16), Aichi virus 3ABC exhibited strong binding ability to the 5′-terminal region of the genome. However, Aichi virus 3AB and 3C did not interact with this region of the genome, unlike those of HAV. Improved RNA binding was not observed even in the presence of both 3AB and 3C (data not shown). The Aichi virus 3C sequence does not contain the presumed RNA-binding motif, KFRDI, which is shared by HAV and some picornavirus 3C proteins (1, 2, 6, 9). The conformation of Aichi virus 3ABC would be important for RNA binding (Fig. 3 and 4).

It has been reported for poliovirus that formation of the RNP complex at the 5′-end region of the genome is required for negative-strand RNA synthesis (5, 13, 19). The 5′-end RNP contains 3CD and PCBP2, both of which interact with PABP that binds to the poly(A) tail, leading to circularization of the genome. In this study, binding analyses involving mutant RNA probes indicated that maintenance of the double-stranded helical region of SL-A and stem-B1 of PK-B is important for interaction with 3ABC (Fig. 6). Maintenance of these helical segments has been shown to be required for negative-strand RNA synthesis (25). In addition, although the efficiency of negative-strand synthesis of mutB-3 has not been examined yet, this mutant, which exhibits decreased RNA replication ability (24), showed reduced binding activity to 3ABC (Fig. 6C and D). Thus, the ability of 3ABC to bind to the 5′-terminal RNA correlated with the RNA replication ability, especially negative-strand synthesis. These results suggest that the interaction of 3ABC with SL-A and stem-B1 of the 5′-terminal element is involved in negative-strand RNA synthesis. To clarify whether Aichi virus 3ABC is involved in genome circularization and whether genome circularization is required for negative-strand synthesis, it appears necessary to examine the interaction of 3ABC with PABP.

On the other hand, disruption of stem-B2 of PK-B and one of the double-stranded segments of SL-C did not abolish the interaction with 3ABC. However, the formation of these structures has previously been shown to be also required for negative-strand RNA synthesis (25). It is likely that stem-B2 and SL-C would be targets for interactions with other viral and/or host proteins responsible for negative-strand synthesis.

Picornaviral RNA synthesis is asymmetric, and positive-strand RNA is synthesized approximately 40- to 70-fold more than negative-strand RNA in infected cells (27). In this study, the in vitro translation analysis using Vero cell extracts showed that 3ABC is a minor processing product (Fig. 2, lanes 3 to 5). It is possible that utilization of a minor product, 3ABC, for negative-strand synthesis is one of the factors for asymmetric RNA synthesis.

It is known that the single-stranded segments in the poliovirus 5′ cloverleaf interact with 3CD and PCBP2 (1, 2, 8, 29). On the other hand, for the interaction between CVB3 3C and the subdomain D of the 5′-terminal cloverleaf structure, the structural features rather than the specific sequence of the loop segment are important (28, 42). The present study indicated that maintenance of the double-stranded stem segment of SL-A and stem-B1 of PK-B is critical for the interaction with Aichi virus 3ABC (Fig. 6). The importance of the nucleotide sequences of the loop segments of SL-A and SL-C in 3ABC binding was not investigated in this study, since the previous studies have shown that nucleotide changes in these loop segments did not affect the virus replication severely (24, 35). The involvement of the specific sequence in the context of a double-stranded structure has been reported for the interaction between poliovirus 2C and the 3′-terminal cloverleaf of negative-strand RNA (3, 4). For SL-A, the nucleotide sequence in the stem segment was not important for the 3ABC binding (Fig. 6A and B). On the other hand, the nucleotide sequence of stem-B1 was found to affect the binding to 3ABC, since the complementary mutation introduced into stem-B1 led to recovery of the binding activity to 3ABC only up to approximately 30% of that of the wild type (Fig. 6C and D).

Northwestern analysis using mutant RNA probes showed that some mutations that do not affect RNA replication reduced the ability to bind to 3CD as severely as did some mutations abolishing RNA replication (Fig. 7). This suggests

that a direct interaction of 3CD with the 5′-terminal region is not required for RNA replication or negative-strand synthesis. In poliovirus, it is thought that 3CD contained in the RNP complex to synthesize negative-strand RNA may provide 3D RNA polymerase by proteolytic cleavage (13, 23). In addition, it is reported that poliovirus 3CD binds not only to the 5′-terminal region but also to the 3′-terminal region of the genome, in the presence of 3AB (12). Although we observed that the presence of 3AB did not improve the binding of Aichi virus 3CD to the 5′-terminal region on gel shift assay (data not shown), it may be necessary to examine further whether 3CD is contained in the RNP complex required for negative-strand synthesis, e.g., through direct interaction with the 3′-terminal region of the genome or through interaction with cellular or viral proteins including 3ABC that bind to the 5′- or 3′-terminal regions.

In conclusion, this study showed that Aichi virus polypeptide 3ABC specifically binds to the 5′-terminal replication element and suggested that the formation of this RNP complex is involved in viral RNA replication, particularly negative-strand RNA synthesis. Thus, although the tertiary structure of the 5′ end of the genome and the viral protein that binds to it are different from those in the case of poliovirus, it is likely that the 5′-terminal structural elements of the Aichi virus genome function in negative-strand RNA synthesis in a similar manner for poliovirus.

ACKNOWLEDGMENT

This work was supported in part by a Grant-in-Aid for Scientific Research and Open Research Center Program from the Ministry of Education, Culture, Sports, Science and Technology of Japan.

REFERENCES

1. **Andino, R., G. E. Rieckhof, and D. Baltimore.** 1990. A functional ribonucleoprotein complex forms around the 5′ end of poliovirus RNA. Cell **63:**369–380.
2. **Andino, R., G. E. Rieckhof, P. L. Achacoso, and D. Baltimore.** 1993. Poliovirus RNA synthesis utilizes an RNP complex formed around the 5′-end of viral RNA. EMBO J. **12:**3587–3598.
3. **Banerjee, R., A. Echeverri, and A. Dasgupta.** 1997. Poliovirus-encoded 2C polypeptide specifically binds to the 3′-terminal sequences of viral negative-strand RNA. J. Virol. **71:**9570–9578.
4. **Banerjee, R., W. Tsai, W. Kim, and A. Dasgupta.** 2001. Interaction of poliovirus-encoded 2C/2BC polypeptides with the 3′ terminus negative-strand cloverleaf requires an intact stem-loop b. Virology **280:**41–51.
5. **Barton, D. J., B. J. O'Donnell, and J. B. Flanegan.** 2001. 5′ cloverleaf in poliovirus RNA is a *cis*-acting replication element required for negative-strand synthesis. EMBO J. **20:**1439–1448.
6. **Bergmann, E. M., S. T. Mosimann, M. M. Chernaia, B. A. Malcolm, and M. N. G. James.** 1997. The refined crystal structure of the 3C gene product from hepatitis A virus: specific proteinase activity and RNA recognition. J. Virol. **71:**2436–2448.
7. **Desvoyes, B., and K.-B. G. Scholthof.** 2000. RNA:protein interactions associated with satellites of panicum mosaic virus. FEBS Lett. **485:**25–28.
8. **Gamarnik, A. V., and R. Andino.** 1997. Two functional complexes formed by KH domain containing proteins with the 5′ noncoding region of poliovirus RNA. RNA **3:**882–892.
9. **Gorbalenya, A. E., A. P. Donchenko, V. M. Blinov, and E. V. Koonin.** 1989. Cysteine proteases of positive strand RNA viruses and chymotrypsin-like serine proteases. FEBS Lett. **243:**103–114.
10. **Graff, J., J. Cha, L. B. Blyn, and E. Ehrenfeld.** 1998. Interaction of poly(rC) binding protein 2 with the 5′ noncoding region of hepatitis A virus RNA and its effects on translation. J. Virol. **72:**9668–9675.
11. **Hämmerle, T., C. U. T. Hellen, and E. Wimmer.** 1991. Site-directed mutagenesis of the putative catalytic triad of poliovirus 3C proteinase. J. Biol. Chem. **266:**5412–5416.
12. **Harris, K. S., W. Xiang, L. Alexander, W. S. Lane, A. V. Paul, and E. Wimmer.** 1994. Interaction of poliovirus polypeptide $3CD^{pro}$ with the 5′ and 3′ termini of the poliovirus genome. J. Biol. Chem. **269:**27004–27014.
13. **Herold, J., and R. Andino.** 2001. Poliovirus RNA replication requires genome circularization through a protein-protein bridge. Mol. Cell **7:**581–591.
14. **Kalinina, N. O., O. N. Fedorkin, O. V. Samuilova, E. Maiss, T. Korpela, S. Y. Morozov, and J. G. Atabekov.** 1996. Expression and biochemical analyses of the recombinant potato virus X 25K movement protein. FEBS Lett. **397:**75–78.
15. **Kusov, Y. Y., G. Morace, C. Probst, and V. Gauss-Müller.** 1997. Interaction of hepatitis A virus (HAV) precursor proteins 3AB and 3ABC with the 5′ and 3′ termini of the HAV RNA. Virus Res. **51:**151–157.
16. **Kusov, Y. Y., and V. Gauss-Muller.** 1997. In vitro RNA binding of the hepatitis A virus proteinase 3C (HAV 3Cpro) to secondary structure elements within the 5′ terminus of the HAV genome. RNA **3:**291–302.
17. **Lawson, M. A., and B. L. Semler.** 1992. Alternate poliovirus nonstructural protein processing cascades generated by primary sites of 3C proteinase cleavage. Virology **191:**309–320.
18. **Leong, L. E. C., P. A. Walker, and A. G. Porter.** 1993. Human rhinovirus-14 protease 3C ($3C^{pro}$) binds specifically to the 5′-noncoding region of the viral RNA. J. Biol. Chem. **268:**25735–25739.
19. **Lyons, T., K. E. Murray, A. W. Roberts, and D. J. Barton.** 2001. Poliovirus 5′-terminal cloverleaf RNA is required in *cis* for VPg uridylylation and the initiation of negative-strand RNA synthesis. J. Virol. **75:**10696–10708.
20. **Martin, L. R., G. M. Duke, J. E. Osorio, D. J. Hall, and A. C. Palmenberg.** 1996. Mutational analysis of the mengovirus poly(C) tract and surrounding heteropolymeric sequences. J. Virol. **70:**2027–2031.
21. **Mason, P. W., S. V. Bezborodova, and T. M. Henry.** 2002. Identification and characterization of a *cis*-acting replication element (*cre*) adjacent to the internal ribosome entry site of foot-and-mouth disease virus. J. Virol. **76:**9686–9694.
22. **Merits, A., D. Guo, and M. Saarma.** 1998. VPg, coat protein and five nonstructural proteins of potato A potyvirus bind RNA in a sequence-unspecific manner. J. Gen. Virol. **79:**3123–3127.
23. **Murray, K. E., and D. J. Barton.** 2003. Poliovirus CRE-dependent VPg uridylylation is required for positive-strand RNA synthesis but not for negative-strand RNA synthesis. J. Virol. **77:**4739–4750.
24. **Nagashima, S., J. Sasaki, and K. Taniguchi.** 2003. Functional analysis of the stem-loop structures at the 5′ end of the Aichi virus genome. Virology **313:**56–65.
25. **Nagashima, S., J. Sasaki, and K. Taniguchi.** 2005. The 5′-terminal region of the Aichi virus genome encodes *cis*-acting replication elements required for positive- and negative-strand RNA synthesis. J. Virol. **79:**6918–6931.
26. **Nateri, A. S., P. J. Hughes, and G. Stanway.** 2002. Terminal RNA replication elements in human parechovirus 1. J. Virol. **76:**13116–13122.
27. **Novak, J. E., and K. Kirkegaard.** 1991. Improved method for detecting poliovirus negative strands used to demonstrate specificity of positive-strand encapsidation and the ratio of positive to negative strands in infected cells. J. Virol. **65:**3384–3387.
28. **Ohlenschläger, O., J. Wöhnet, E. Bucci, S. Seitz, S. Häfner, R. Ramachandran, R. Zell, and M. Görlach.** 2004. The structure of the stemloop D subdomain of coxsackievirus B3 cloverleaf RNA and its interaction with the proteinase 3C. Structure **12:**237–248.
29. **Parsley, T. B., J. S. Towner, L. B. Blyn, E. Ehrenfeld, and B. L. Semler.** 1997. Poly (rC) binding protein 2 forms a ternary complex with the 5′-terminal sequences of poliovirus RNA and the viral 3CD proteinase. RNA **3:**1124–1134.
30. **Percy, N., W. S. Barclay, M. Sullivan, and J. W. Almond.** 1992. A poliovirus replicon containing the chloramphenicol acetyltransferase gene can be used to study the replication and encapsidation of poliovirus RNA. J. Virol. **66:**5040–5046.
31. **Peters, H., Y. Y. Kusov, S. Meyer, A. J. Benie, E. Bäuml, M. Wolff, C. Rademacher, T. Peters, and V. Gauss-Müller.** 2005. Hepatitis A virus proteinase 3C binding to viral RNA: correlation with substrate binding and enzyme dimerization. Biochem. J. **385:**363–370.
32. **Pringle, C. R.** 1999. Virus taxonomy at the XIth International Congress of Virology, Sydney, Australia, 1999. Arch. Virol. **144:**2065–2070.
33. **Racaniello, V. R.** 2001. Picornaviridae: the viruses and their replication, p. 685–722. *In* D. M. Knipe, P. M. Howley, D. E. Griffin, R. A. Lamb, M. A. Martin, B. Roizman, and S. E. Straus (ed.), Fields virology, 4th ed. Lippincott/The Williams & Wilkins Co., Philadelphia, PA.
34. **Rohll, J. B., N. Percy, R. Ley, D. J. Evans, J. W. Almond, and W. S. Barclay.** 1994. The 5′-untranslated regions of picornavirus RNAs contain independent functional domains essential for RNA replication and translation. J. Virol. **68:**4384–4391.
35. **Sasaki, J., Y. Kusuhara, Y. Maeno, N. Kobayashi, T. Yamashita, K. Sakae, N. Takeda, and K. Taniguchi.** 2001. Construction of an infectious cDNA clone of Aichi virus (a new member of the family *Picornaviridae*) and mutational analysis of a stem-loop structure at the 5′ end of the genome. J. Virol. **75:**8021–8030.
36. **Sasaki, J., and K. Taniguchi.** 2003. The 5′-end sequence of the genome of Aichi virus, a picornavirus, contains an element critical for viral RNA encapsidation. J. Virol. **77:**3542–3548.
37. **Schultheiss, T., Y. Y. Kusov, and V. Gauss-Müller.** 1994. Proteinase 3C of

hepatitis A virus (HAV) cleaves the HAV polyprotein P2-P3 at all sites including VP1/2A and 2A/2B. Virology **198:**275–281.

38. **Walker, P. A., L. E.-C. Leong, and A. G. Porter.** 1995. Sequence and structural determinants of the interaction between the 5′-noncoding region of picornavirus RNA and rhinovirus. J. Biol. Chem. **270:**14510–14516.
39. **Xiang, W., K. S. Harris, L. Alexander, and E. Wimmer.** 1995. Interaction between the 5′-terminal cloverleaf and 3AB/3CD^{pro} of poliovirus is essential for RNA replication. J. Virol. **69:**3658–3667.
40. **Yamashita, T., S. Kobayashi, K. Sakae, S. Nakata, S. Chiba, Y. Ishihara, and S. Isomura.** 1991. Isolation of cytopathic small round viruses with BS-C-1 cells from patients with gastroenteritis. J. Infect. Dis. **164:**954–957.
41. **Yamashita, T., K. Sakae, H. Tsuzuki, Y. Suzuki, N. Ishikawa, N. Takeda, T. Miyamura, and S. Yamazaki.** 1998. Complete nucleotide sequence and genetic organization of Aichi virus, a distinct member of the *Picornaviridae* associated with acute gastroenteritis in humans. J. Virol. **72:**8408–8412.
42. **Zell, R., K. Sidigi, E. Bucci, A. Stelzner, and M. Gorlach.** 2002. Determinants of the recognition of enteroviral cloverleaf RNA by coxsackievirus B3 proteinase 3C. RNA **8:**188–201.